A MIMO Channel Measurement System Based on Delay Lines and Simulations Based on Graph Modeling

Shengnan Xu(✉)

Tongji University, Shanghai, China
1832953@tongji.edu.cn

Abstract. In this paper, we proposed a novel MIMO channel measurement system architecture for 5G wireless communication based on the delay lines in combination with switches, and we implement propagation graph modeling to simulate the channel measurement procedure. Channel sounders equipped with multiple-element antenna arrays in the transmitter (Tx) and receiver (Rx) usually perform a measurement in two ways: switched channel measurement and parallel channel measurement. The latter usually needs multiple Txs/Rxs which leads a high cost, while the former with a high-speed radio-frequency switch at the transmitter and receiver has a lower cost but it is difficult to realize beamforming due to the Tx/Rx antennas do not transmit/receive signals simultaneously. By adding delay lines to the switched MIMO channel measurement system, the delay in different time slot at every Tx antennas can be compensated so that the multiple Tx antennas (empowered by only one Tx) transmit signals simultaneously. Furthermore, adding phase shifters after delay lines makes it easy to change the phase of each signal, which provides a convenient way for beamforming. The feasibility of the proposed method is preliminarily validated through simulations based on propagation graph modeling, the evaluation of the results is conducted by calculating the channel impulse response (CIR) or power delay profile (PDP) and estimating the direction of arrival (DOA) using Multiple Signal Classification (MUSIC) algorithm.

Keywords: Channel measurement · Delay line · Switch · Propagation graph modeling

1 Introduction

In the development of wireless communication, the evolution of each generation of communication systems is accompanied by an ascent in frequency and bandwidth. The fifth Generation (5G) wireless communication systems will use channels with bandwidth up to 0.5–2 GHz to offer sufficient spectral resources for the users in the frequency range of 0.45–85 GHz [1]. The accurate description of the propagation channel characteristics is the basis of design, analysis and optimization of the 5G wireless communication system. Channel measurement need to be performed accurately. In addition to that, new techniques and scenarios of the 5G wireless communication, such

H. Gao et al. (Eds.): ChinaCom 2020, LNICST 352, pp. 189–199, 2021.
https://doi.org/10.1007/978-3-030-67720-6_13

as massive MIMO, beamforming and millimeter wave communication, require new methodology for channel measurement.

Massive MIMO is a key technique for 5G, which requires a large number of antennas, for example, 32 antennas, 64 antennas, or even more. In this scenario, traditional parallel channel measurement needs a large number of transmitters (TXs). Switched channel measurement is an alternative, but it is inconvenient to implement beamforming, due to it is a time-division-multiplexing (TDM) measurement scheme.

Many schemes for high-frequency channel measurement have been studied. In [2], the authors performed a channel measurement campaign in the frequency domain based on VNA (vector network analyzer), in which the transmitter uses optical fiber for transmission to increase the measurement distance of the VNA-based system. [3] presents a time-domain channel measurement system using a spread spectrum sliding correlator method. The sliding correlator achieves superior multipath time resolution and dynamic range by using pseudo noise sequences operated at slightly different clock speeds at the transmitter and receiver, but it is hard to be extended to multi-band measurement for it is only applicable to fixed frequency bands. It is well known that the multi-antenna channel measurement and the acquisition of spatial angle information are particularly important, and [4] introduces a 28 GHz channel sounder based on automatically rotating horn antennas with time synchronization ability between the transmitter and the receiver. The sounder system in [4] realize a virtual array and the use of high-gain narrow-beam directional antennas compensates the severe attenuation of the millimeter wave channel. [5] presents a novel MIMO channel sounding technique with a fully parallel transceiver architecture that employs a layered scheme of frequency and space-time division multiplexing, and it offers inherent scalability of the number of antennas by a combination of multiple transceiver units and exhibits flexibility for both directional MIMO channel and multi-link MIMO channel measurements. In [6–8], some researches focus on exploring higher efficiency and lower cost MIMO channel measurement systems.

Besides the measurement-based researches, simulation-based methods for channel measurement and modeling are also worth studying. In fact, simulation-based methods become popular in 5G scenarios due to the advantages in efficiency, flexibility and low cost. Graph theory based channel modeling has proved to be an effective approach to simulate the multipath propagation and the diffuse components, which means it is promising to simulate the radio propagation in highly diffuse scattering conditions like propagation at the millimeter wave. It is well known that propagation graph modeling is a good alternative to measurement campaign in environments which are difficult to perform actual measurement, such as the high-speed railway propagation environments. The applicability of graph modeling in high-speed railway propagation environments has been proved in [9]. In [10], the stochastic graph modeling approach is assessed by comparing the statistical characteristics of the channel parameters acquired from graph modeling in an indoor environment with the parameters specified in established WINNER II channel models. In [11], authors proposed a deterministic graph modeling approach by associating the scatterers with realistic environment objects, and by calculating the coefficients of propagation paths based on a proven diffuse scattering theory.

In this paper, we proposed a MIMO channel measurement system with only one Tx/Rx for 5G wireless communication based on delay lines in combination with switches aiming at overcoming the shortcoming that traditional switched channel measurement cannot transmit or receive signals simultaneously which obstructs the realization of beamforming. Then we implement stochastic propagation graph modeling to simulate the channel measurement procedure. In the simulation, delay lines were added to the transmitter to realize transmitting signals simultaneously. The channel impulse response can be calculated analytically with limited computational cost, and we estimate the direction of arrival (DOA) using MUSIC algorithm. The organization of this paper is as follows: Sect. 2 introduces the schematic of the proposed measurement systems and the procedure of simulations for the proposed measurement system. A brief introduction for the graph theory based modeling is also presented. In Sect. 3, the analysis of simulation results is given. Finally, conclusive remarks are addressed in Sect. 4.

2 Simulations for the Proposed Measurement System Based on Graph Modeling

2.1 The Structure of Proposed Measurement System

The structure of proposed MIMO channel measurement system is shown in Fig. 1, the transmitter is equipped with delay lines connecting the switches and phase shifters that help to implement beamforming, hence, the measurement system can transmit signals simultaneously only with one channel sounder and is friendly to beamforming. Antenna arrays at the receiver receive signals parallelly without extra devices as a normal multiple-output.

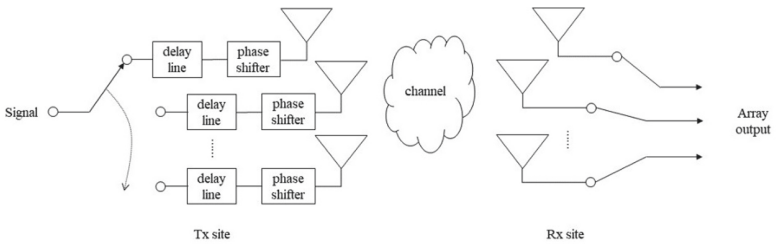

Fig. 1. The structure of proposed MIMO channel measurement system.

2.2 Basic Theory of Propagation Graph Modeling

The propagation graph modeling proposed in [12] calculates the transfer function as:

$$\mathbf{H}(f) = \mathbf{D}(f) + \mathbf{R}(f)(\mathbf{I} - \mathbf{B}(f))^{-1}\mathbf{T}(f) \tag{1}$$

where $\mathbf{D}(f)$ represents the Line-of-Sight (LoS) component of the transfer function and the other terms are the None-Line-of-Sight (NLOS) components of the transfer function. In detail, $\mathbf{D}(f)$ denotes the matrix of the transfer function from the Tx to the Rx directly and $\mathbf{B}(f)$ denotes the bouncing matrix of the transfer function between the scatters, $\mathbf{T}(f)$ and $\mathbf{R}(f)$ denote the matrices of the transfer function from the Tx to the scatters and from the scatters to the Rx, respectively. Detailed derivation of (1) and more information about propagation graph modeling can refer to [12]. The transfer function of a propagation path can be calculated as:

$$A_e(f) = g_e(f)\exp(-j2\pi\tau_e f + j\varphi) \tag{2}$$

where $A_e(f)$ represents the elements of matrices $\mathbf{D}(f)$, $\mathbf{R}(f)$, $\mathbf{B}(f)$ and $\mathbf{T}(f)$ according to different kinds of edges, τ_e denotes the propagation delay between two vertices, and φ is a random phase rotation considered as a random variable uniformly distributed on the interval $[0, 2\pi)$, and $g_e(f)$ is the propagation coefficient depends on different kinds of edges. $g_e(f)$ was originally defined in [13], and a modified deterministic definition of $g_e(f)$ was proposed in [14].

2.3 Procedure of the Simulation

The steps for the simulation of the channel measurement system based on graph modeling in a given propagation environment are generally elaborated as follows:

Step 1: Set the vertex information of the polygonal surfaces according to the digital map of the given environment, and set the positions of the transmitters and receivers as we want;

Step 2: Generate the positions of the scatterers by discretize every object surface into multiple scatterers, record the coordinates of the scatterers, and the normal directions of the surfaces are also recorded and assigned to the corresponding scatterers;

Step 3: Judge the visibility for every pair of two vertices (i.e. a Tx and a scatterer, a scatterer and a Rx) according to their positions and the positions of the other scatterers, which can be implemented by the method that judges whether the edge connecting the two vertices intersects the other scatterers. A propagation graph is now build up, Fig. 2 shows an example of digital map;

Step 4: Calculate the propagation coefficient $g_e(f)$ for each available link and generate the matrices $\mathbf{D}(f)$, $\mathbf{R}(f)$, $\mathbf{B}(f)$ and $\mathbf{T}(f)$ according to (2) for specific frequencies $f = f_{min}, f_{min} + \Delta f, \ldots, f_{max}$;

Step 5: Embed the antenna radiation pattern for the matrices $\mathbf{T}(f)$ and $\mathbf{R}(f)$, here we use omnidirectional antenna radiation pattern;

Step 6: Add time delays to each transmitted signal by adding a delay $(k-1)\tau$ to every element of kth column vector of both $\mathbf{D}(f)$ and $\mathbf{T}(f)$ to simulate the extra delay caused by switches, which means the $A_e(f)$ in both $\mathbf{D}(f)$ and $\mathbf{T}(f)$ change as follow:

$$A_{e,k}(f) = g_{e,k}(f)\exp\left(-j2\pi\left(\tau_{e,k} + (k-1)\tau\right)f + j\varphi\right) \tag{3}$$

where $A_{e,k}(f)$ denotes the elements of kth column vector of $\mathbf{D}(f)$ and $\mathbf{T}(f)$. Then we use $\mathbf{D}'(f)$ and $\mathbf{T}'(f)$ to represent $\mathbf{D}(f)$ and $\mathbf{T}(f)$ after adding time delays, respectively.

Step 7: According to (1), $\mathbf{D}'(f)$, $\mathbf{R}(f)$, $\mathbf{B}(f)$ and $\mathbf{T}'(f)$ are used to calculate the channel transfer function $\mathbf{H}'(f)$ with delays caused by switches, and replace $\mathbf{D}'(f)$ and $\mathbf{T}'(f)$ with $\mathbf{D}(f)$ and $\mathbf{T}(f)$ respectively, we get the channel transfer function $\mathbf{H}(f)$ with delays compensated by delay lines. The CIR is the inverse Fourier transform of the transfer function.

The above procedure shows how to simulate the measurement process based on delay lines and switches. The whole modeling is similar to the original graph modeling procedure [14], however, the processing of calculating CIR is a little different. Finally, we acquire the direction information from CIR adopting MUSIC algorithm.

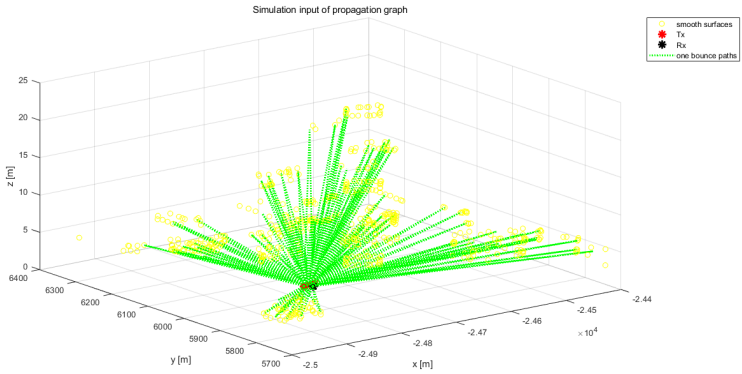

Fig. 2. An example of digital map in simulations.

3 Results of the Simulation

Delay lines are usually tunable in a certain range, but it is still a little difficult to implement the phase shift of a signal by adjusting delay lines, hence we employ the phase shifter as a helper for beamforming after the switch delays compensated by delay lines. Here we consider an N-element linear array composed of isotropic radiating antenna elements, and it is assumed that the signal of the nth element is added with a phase shift $(n-1)\delta$ by tuning the phase shifter. Additionally, we assume the carrier frequency as $f = 1.75$ GHz, and the spacing of the elements as $d = \lambda/2$ (λ is the wave length). Here, we add different δ to an 8-element linear array ($N = 8$), and the corresponding array factor patterns are exhibited in Fig. 3, 4 and 5. Figure 3 shows the original array factor pattern at $\delta = 0$, while $\delta = \pi/2$ and π respectively in Fig. 4 and 5. Obviously, the three patterns are different from each other. For different δ, adding phase shift $(n-1)\delta$ on the nth array element after the switch delays compensated by delay lines changes the array factor pattern, which means that beamforming is likely to be realized conveniently. The method of embedding phase shift δ into $\mathbf{D}(f)$ and $\mathbf{T}(f)$ is similar to the step 6 in Sect. 2.3, and we have an expression similar to (3):

$$A_{e,k}(f) = g_{e,k}(f)\exp(-j(2\pi\tau_{e,k}f + (k-1)\delta) + j\varphi) \tag{4}$$

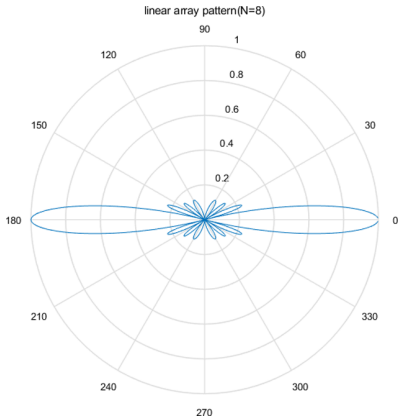

Fig. 3. Array factor patterns with $\delta = 0$.

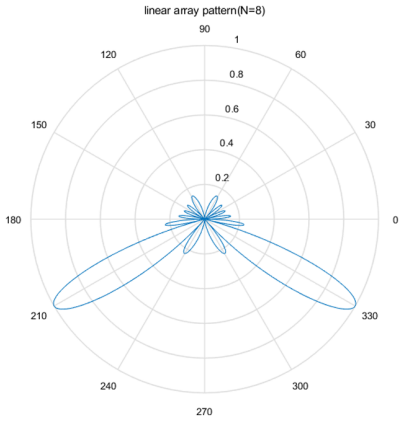

Fig. 4. Array factor patterns with $\delta = \pi/2$.

Then following the steps in Sect. 2.3, simulations were conducted. The configuration of simulations is described as follows: 3 Tx antennas, 20 Rx antennas, frequency band of 1.74–1.76 GHz with 51 frequency points, the interval of Tx antennas is $\lambda/2$ (λ is the wave length of the carrier), while the interval of Rx antennas is $\lambda/4$, and the relationship of positions of the Tx antennas and Rx antennas is shown in Fig. 6, the switch interval $\tau = 57$ ns (the value of τ can be set according to the actual radio-frequency switch). PDPs are obtained easily from the graph modeling transfer function $\mathbf{H}(f)$ or $\mathbf{H}'(f)$, Fig. 7 and 8 show the PDPs acquired from the simulation that has delays caused by radio-frequency switches. Figure 7 is the PDP about the signal component from each Tx antenna to each Rx antenna including 60 curves, and Fig. 8 shows the PDP of the signal component from each Tx antenna to all Rx antennas including 3 curves. It is obvious that main peaks in the PDPs appear respectively at different positions about 50 ns, 100 ns and 150 ns, which means there are fixed delays existing

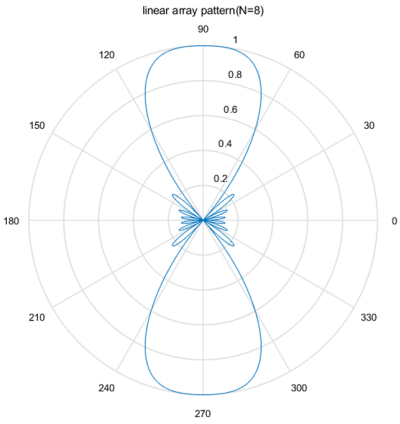

Fig. 5. Array factor patterns with $\delta = \pi$

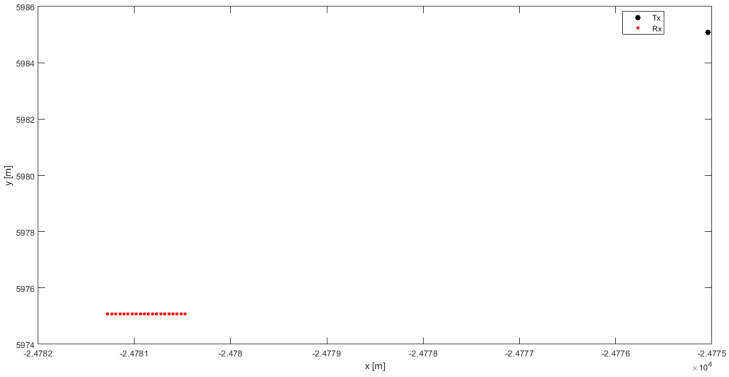

Fig. 6. Positions of Tx antennas and Rx antennas.

in signals transmitted by different Tx antennas. By introducing the delay lines, the fixed time delay of transmitting signals can be compensated. The results of the simulation with delay lines are shown in Fig. 9 and 10, where Fig. 9 describes the PDP of the signal component from each Tx antenna to each Rx antenna and Fig. 10 illustrates the PDP of the signal component from each Tx antenna to all Rx antennas. Both Fig. 9 and 10 display the coincident main peaks at about 50 ns, which reflects the effect brought by delay lines.

For validating the effect of beamforming, phase shift $(n - 1)\delta$ is embedded into the nth Tx antenna under the condition that switch delays are compensated using delay lines, and then MUSIC algorithm is used to estimate the DOA of the simulations. Here we only estimate the azimuth of arrival (AOA) ignoring the elevation of arrival for simplification purpose, and it is reasonable to be based on the premise that the Tx antennas and Rx antennas are almost at the same height. We set $\delta = \pi/2$, and according to the array factor pattern presented in Fig. 4 (the pattern of 3-element linear array we

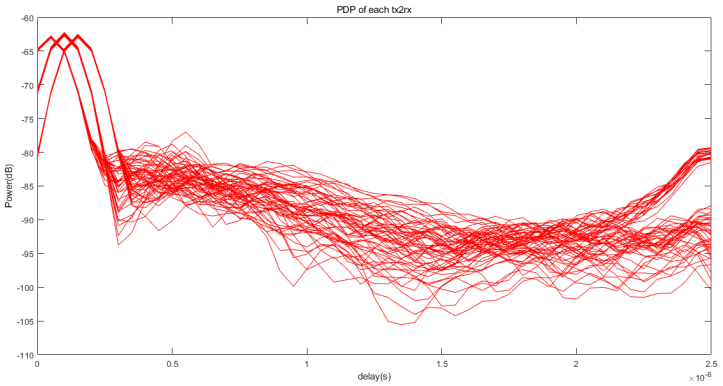

Fig. 7. PDP of the signal component of each Tx to each Rx with delays caused by switches.

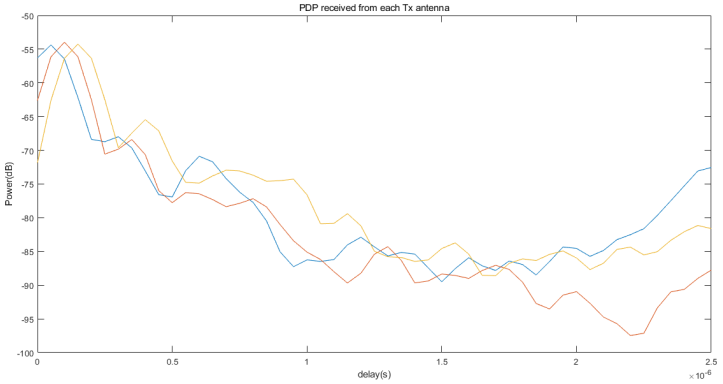

Fig. 8. PDP of the signal component from each Tx antenna with delays caused by switches.

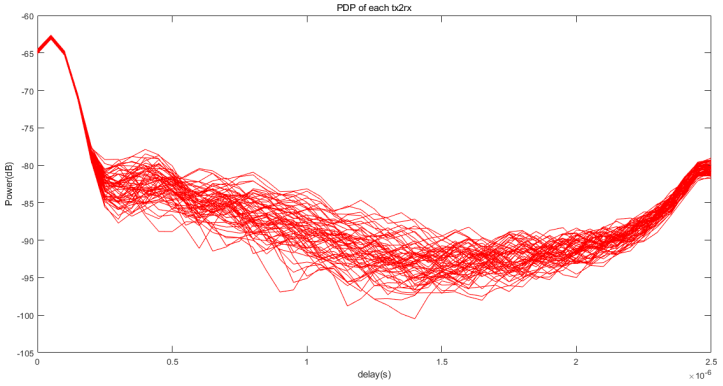

Fig. 9. PDP of the signal component of each Tx to each Rx when delays compensated by delay lines.

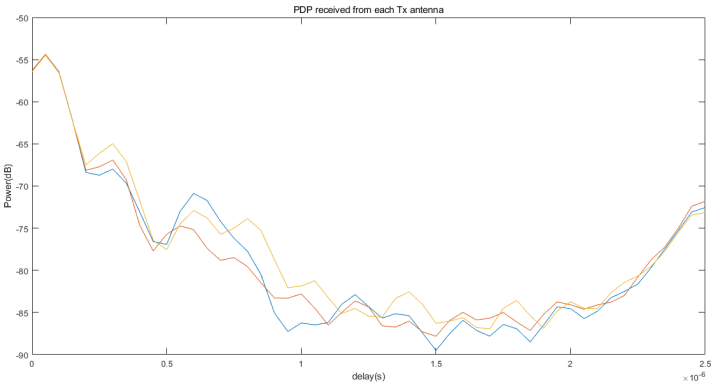

Fig. 10. PDP of the signal component from each Tx antenna when delays compensated by delay lines.

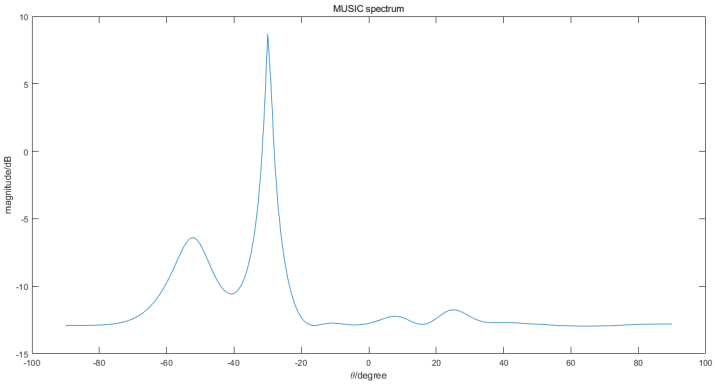

Fig. 11. MUSIC spectrum with delay lines and phase shifter.

adopted is similar) and the positions of Tx and Rx, the AOA is about −30° or −150° theoretically. The estimate results are shown in Fig. 11. We can see that a high peak appears at about −30° in the MUSIC spectrum, which conforms to the theoretical result. Additionally, there is a little peak at about −55°. We consider it reasonable for which the peak is really low and the array pattern with $\delta = \pi/2$ shown in Fig. 4 has a side lobe at −60°. In some way, the simulation results preliminarily prove that the proposed MIMO measurement scheme is applicable.

4 Conclusion

In this paper, we have proposed a MIMO channel measurement system for wireless communication based on delay lines associating with switches. Compared to the traditional switched channel measurement system, the proposed measurement system

changes the time-division-multiplexing sounding method adopted by the traditional system. Combining delay lines with switches realizes that multiple Tx antennas transmit signals simultaneously only with one channel sounder in a low-cost way, which also provides a convenient way to beamforming. Simulations for this measurement system based on propagation graph modeling have been implemented, and the results preliminarily show that this MIMO channel measurement system has an applicable potential to channel measurement.

References

1. Ngo, H.Q., Larsson, E.G., Marzetta, T.L.: Energy and spectral efficiency of very large multiuser MIMO systems. IEEE Trans. Commun. **61**(4), 1436–1449 (2013)
2. Naderpour, R., Vehmas, J., Nguyen, S., Järveläinen, J., Haneda, K.: Spatio-temporal channel sounding in a street canyon at 15, 28 and 60 GHz. In: 2016 IEEE 27th Annual International Symposium on Personal, Indoor, and Mobile Radio Communications (PIMRC), Valencia, pp. 1–6 (2016)
3. Ben-Dor, E., Rappaport, T.S., Qiao, Y., Lauffenburger, S.J.: Millimeter-wave 60 GHz outdoor and vehicle AOA propagation measurements using a broadband channel sounder. In: 2011 IEEE Global Telecommunications Conference-GLOBECOM 2011, Houston, TX, USA, pp. 1–6 (2011)
4. Hur, S., Cho, Y., Lee, J., Kang, N.-G., Park, J., Benn, H.: Synchronous channel sounder using horn antenna and indoor measurements on 28 GHz. In: 2014 IEEE International Black Sea Conference on Communications and Networking (BlackSeaCom), Odessa, pp. 83–87 (2014)
5. Kim, M., Takada, J., Konishi, Y.: Novel scalable MIMO channel sounding technique and measurement accuracy evaluation with transceiver impairments. IEEE Trans. Instrum. Measur. **61**(12), 3185–3197 (2012)
6. Papazian, P.B., Gentile, C., Remley, K.A., Senic, J., Golmie, N.: A radio channel sounder for mobile millimeter-wave communications: system implementation and measurement assessment. IEEE Trans. Microwave Theory Tech. **64**(9), 2924–2932 (2016)
7. Salous, S., Feeney, S.M., Raimundo, X., Cheema, A.A.: Wideband MIMO channel sounder for radio measurements in the 60 GHz band. IEEE Trans. Wireless Commun. **15**(4), 2825–2832 (2016)
8. Müller, R., et al.: Simultaneous multi-band channel sounding at mm-Wave frequencies. In: 2016 10th European Conference on Antennas and Propagation (EuCAP), Davos, pp. 1–5 (2016)
9. Tian, L., Yin, X., Zuo, Q., Zhou, J., Zhong, Z., Lu, S.X.: Channel modeling based on random propagation graphs for high speed railway scenarios. In: 2012 IEEE 23rd International Symposium on Personal, Indoor and Mobile Radio Communications-(PIMRC), Sydney, NSW, pp. 1746–1750 (2012)
10. Tian, L., Yin, X., Zhou, X., Zuo, Q.: Spatial cross-correlation modeling for propagation channels in indoor distributed antenna systems. EURASIP J. Wireless Commun. Netw. **2013** (1), 1–11 (2013). https://doi.org/10.1186/1687-1499-2013-183
11. Tian, L., Degli-Esposti, V., Vitucci, E.M., Yin, X., Mani, F., Lu, S.X.: Semi-deterministic modeling of diffuse scattering component based on propagation graph theory. In: 2014 IEEE 25th Annual International Symposium on Personal, Indoor, and Mobile Radio Communication (PIMRC), Washington, DC, pp. 155–160 (2014)

12. Pedersen, T., Fleury, B.H.: Radio channel modelling using stochastic propagation graphs. In: 2007 IEEE International Conference on Communications, Glasgow, pp. 2733–2738 (2007)
13. Pedersen, T., Steinbock, G., Fleury, B.H.: Modeling of reverberant radio channels using propagation graphs. IEEE Trans. Antennas Propag. **60**(12), 5978–5988 (2012)
14. Tian, L., Degli-Esposti, V., Vitucci, E.M., Yin, X.: Semi-deterministic radio channel modeling based on graph theory and ray-tracing. IEEE Trans. Antennas Propag. **64**(6), 2475–2486 (2016)